

# Achieving double-logarithmic precision dependence in optimization-based quantum unstructured search

Zhijian Lai,<sup>1</sup> Dong An,<sup>1</sup> Jiang Hu,<sup>2</sup> and Zaiwen Wen<sup>1</sup>

<sup>1</sup>*Beijing International Center for Mathematical Research, Peking University, Beijing, China*

<sup>2</sup>*Yau Mathematical Sciences Center, Tsinghua University, Beijing, China*

(Dated: March 30, 2026)

Grover’s algorithm is a fundamental quantum algorithm that achieves a quadratic speedup for unstructured search problems of size  $N$ . Recent studies have reformulated this task as a maximization problem on the unitary manifold and solved it via linearly convergent Riemannian gradient ascent (RGA) methods, resulting in a complexity of  $\mathcal{O}(\sqrt{N} \log(1/\varepsilon))$ . In this work, we adopt the Riemannian modified Newton (RMN) method to solve the quantum search problem. We show that, in the setting of quantum search, the Riemannian Newton direction is collinear with the Riemannian gradient in the sense that the Riemannian gradient is always an eigenvector of the corresponding Riemannian Hessian. As a result, without additional overhead, the proposed RMN method numerically achieves a quadratic convergence rate with respect to error  $\varepsilon$ , implying a complexity of  $\mathcal{O}(\sqrt{N} \log \log(1/\varepsilon))$ , which is double-logarithmic in precision. Furthermore, our approach remains Grover-compatible, namely, it relies exclusively on the standard Grover oracle and diffusion operators to ensure algorithmic implementability, and its parameter update process can be efficiently precomputed on classical computers.

## I. INTRODUCTION

Unstructured search, the task of finding specific target elements in an unsorted space of size  $N$ , is a ubiquitous challenge across cryptographic analysis [1, 2], optimization [3, 4], and machine learning [5, 6]. Classically, this problem is inherently inefficient, as guaranteeing success requires  $\Omega(N)$  queries [7]. This constitutes a severe computational bottleneck for large-scale data retrieval [8, 9].

Grover’s quantum search algorithm resolved this bottleneck by achieving an optimal query complexity of  $\Theta(\sqrt{N})$  [10–13], marking a landmark demonstration of quantum advantage. Beyond its direct application to the search problem, Grover’s mechanism is a fundamental primitive in quantum computing. Its principles form the basis of amplitude amplification [14, 15] and have been further generalized within the broader framework of quantum singular value transformation (QSVT) [16, 17].

To gain deeper insights into the mechanics of Grover’s quadratic speedup, researchers have explored various mathematical interpretations. Early efforts characterized Grover’s iteration as a geodesic in complex projective space [18]. Other perspectives have used information geometry to describe the algorithm as a path under the Wigner-Yanase metric [19], while recent work has proposed a connection to imaginary-time evolution (ITE) [20]. These interpretations link the efficiency of quantum search to the geometry of the quantum state space.

A promising modern approach to analyzing such quantum processes is the (*Riemannian*) *manifold optimization* framework [21–23]. Since quantum operations are constrained by unitarity, they naturally lie on the unitary manifold, namely, the unitary group  $\{U \in \mathbb{C}^{N \times N} | U^\dagger U = I\}$  [24]. Formulating various quantum tasks as optimization problems on these Riemannian manifolds has led to significant progress in quantum tomography [25, 26],

ground-state preparation [27–31], Hamiltonian simulation [32, 33], and circuit compilation [34–36].

Specifically, a recent study [37] reformulates Grover’s search as a maximization problem on the unitary manifold and proposes a physically implementable *Riemannian gradient ascent* (RGA) method to achieve the desired quadratic speedup in size  $N$ . While this first-order approach establishes a rigorous link between the optimization framework and quantum dynamics, it is limited to linear convergence with respect to the accuracy parameter  $\varepsilon$ , with total complexity  $\mathcal{O}(\sqrt{N} \log(1/\varepsilon))$ .

To further accelerate convergence in terms of the target accuracy  $\varepsilon$ , second-order optimization methods, such as the Riemannian Newton method [21, 38], provide a natural approach. In this work, we propose a tailored *Riemannian modified Newton* (RMN) method for Grover’s search problem, where each iteration admits a physically implementable second-order update using only the oracle and diffusion operators, analogous to Grover’s algorithm.

Typically, moving from first-order methods to second-order methods trades faster convergence for higher computational cost per iteration, often due to Hessian inversion. A key theoretical result of our RMN method is that the Riemannian gradient of our cost function in unstructured search is always an eigenvector of the associated Riemannian Hessian. This implies that the Newton direction reduces to a scaled gradient, eliminating the need for explicit Hessian inversion. Consequently, second-order updates incur no additional overhead compared to first-order updates.

We test our RMN method numerically and find that, once the iterates get close to the target state, RMN can attain very high-precision solutions in very few iterations. Furthermore, our numerical results show that RMN achieves a quadratic convergence rate with respect to the accuracy  $\varepsilon$ , with total complexity  $\mathcal{O}(\sqrt{N} \log \log(1/\varepsilon))$ . Our work advances the optimization-based framework for

quantum algorithm design.

*a. Organization.* In Section II, we introduce the preliminaries of the unstructured search problem. In Section III, we revisit the Grover-compatible Riemannian gradient ascent method. In Section IV, we derive the Riemannian Hessian and present the proposed Grover-compatible Riemannian modified Newton method. Numerical experiments are provided in Section V. We conclude in Section VI.

## II. PRELIMINARIES

We first review the notation for the unstructured search problem and then reformulate it as a maximization problem on the unitary manifold, followed by a discussion of the corresponding optimality conditions. In the subsequent sections, we will propose several algorithms.

### A. Problem statement

Let  $\mathcal{H}$  be the  $N$ -dimensional Hilbert space of an  $n$ -qubit system with  $N = 2^n$ . We consider an unstructured search problem over the finite set  $[N] := \{0, 1, \dots, N-1\}$ , where a binary oracle function  $g: [N] \rightarrow \{0, 1\}$  specifies whether an element is marked. The set of marked items is  $S := \{x \in [N] : g(x) = 1\}$  with  $M := |S|$  and typically  $1 \leq M \ll N$ . The goal of the search task is to identify at least one element in  $S$ .

Let  $\{|j\rangle\}_{j=0}^{N-1}$  denote the computational basis of  $\mathcal{H}$ , where  $|j\rangle$  represents the  $j$ -th standard basis vector. Define the marked subspace as  $\mathcal{T} := \text{span}_{\mathbb{C}}\{|x\rangle : x \in S\} \subseteq \mathcal{H}$ . The quantum search algorithm can then be interpreted as the task of preparing a normalized state vector in  $\mathcal{T}$ . Let the orthogonal projector onto  $\mathcal{T}$  be

$$H := \sum_{x \in S} |x\rangle\langle x|. \quad (1)$$

Grover's algorithm begins with the uniform superposition over the entire computational basis, i.e.,  $|\psi_0\rangle := \frac{1}{\sqrt{N}} \sum_{x=0}^{N-1} |x\rangle$ . We denote the associated rank-one projector by  $\psi_0 := |\psi_0\rangle\langle\psi_0|$ . Grover's algorithm uses two types of quantum gates, the *diffusion* operator and the *oracle* operator, defined respectively as

$$\begin{aligned} D(\alpha) &:= e^{i\alpha\psi_0} = I + (e^{i\alpha} - 1)\psi_0, \\ O_g(\beta) &:= e^{i\beta H} = I + (e^{i\beta} - 1)H, \end{aligned} \quad (2)$$

where the parameters  $\alpha, \beta \in \mathbb{R}$  denote the angles. Grover iterations are constructed by alternating these two operators,  $G(\alpha_k, \beta_k) = -D(\alpha_k)O_g(\beta_k)$ . After  $T$  iterations, the resulting state is  $|\psi_{\text{final}}\rangle = \prod_{k=1}^T G(\alpha_k, \beta_k) |\psi_0\rangle$ , which aims to approximate the ideal target state

$$|\psi^*\rangle := \frac{1}{\sqrt{M}} \sum_{x \in S} |x\rangle \in \mathcal{T}. \quad (4)$$

The query complexity of Grover's algorithm is commonly measured by the number of oracle calls  $O_g(\beta) = e^{i\beta H}$ . Detailed circuit implementations of both gates can be found in standard textbooks [11, 39].

In the original version of Grover's algorithm [10], the parameters are chosen as  $\alpha_k = \beta_k = \pi$  for all  $k$ . However, this choice may lead to the overshooting problem [40]: performing too many Grover iterations may cause the state to rotate past the target rather than toward it. To mitigate this issue, the  $\pi/3$  algorithm [41] fixes the angles at  $\alpha_k = \beta_k = \pi/3$ , although this modification loses the quadratic speedup. Later, the fixed-point algorithm [42] was proposed to avoid overshooting while still retaining the quadratic speedup.

### B. Manifold optimization formulation

In this subsection, we reformulate the quantum search problem as a maximum-eigenstate preparation problem, which can further be cast as a manifold optimization problem. This idea has been proposed in [20, 37]. Throughout, we equip the matrix space with the Frobenius inner product  $\langle A, B \rangle := \text{Tr}(A^\dagger B)$ .

Let us consider the Hamiltonian  $H$  defined in (1). It satisfies  $H = H^\dagger = H^2$ , which implies that its eigenvalues can only take the values 0 and 1. In fact, the spectrum of  $H$  consists of eigenvalue 1 on the marked subspace  $\mathcal{T}$  with multiplicity  $M$ , and eigenvalue 0 on its orthogonal complement  $\mathcal{T}^\perp$ . In particular, we have  $H|\psi^*\rangle = |\psi^*\rangle$ .

Let  $q_0 := \frac{M}{N} \in (0, 1)$  denote the probability of selecting a marked item at random. Applying  $H$  to the initial state gives  $H|\psi_0\rangle = \sqrt{q_0}|\psi^*\rangle$ . Thus, the initial expectation value satisfies  $\langle\psi_0|H|\psi_0\rangle = \|H|\psi_0\rangle\|^2 = \|\sqrt{q_0}|\psi^*\rangle\|^2 = q_0$ . Indeed, for any state  $|\psi\rangle$ , the expectation value  $\langle\psi|H|\psi\rangle = \sum_{x \in S} |\langle x|\psi\rangle|^2 \in [0, 1]$  represents the probability of observing a marked item when measuring  $|\psi\rangle$  in the computational basis.

Based on the above discussion, our goal now is to construct a quantum state whose expectation value with respect to  $H$  (i.e., the probability of observing a marked item) equals 1. To achieve this, we start from an easily prepared state  $|\psi_0\rangle$  and aim to design a quantum circuit  $U$ , whose quantum gates are easily implementable on quantum hardware (e.g., diffusion/oracle operators), such that the resulting state  $U|\psi_0\rangle$  becomes an eigenstate of  $H$  corresponding to its largest eigenvalue 1.

Consequently, we consider the following manifold optimization problem:

$$\max_{U \in \text{U}(N)} f(U), \quad (5)$$

where the feasible region is the compact Lie group of  $N \times N$  unitary matrices, which forms a Riemannian manifold,

$$\text{U}(N) := \{U \in \mathbb{C}^{N \times N} \mid U^\dagger U = I_N\}, \quad (6)$$

and the cost function  $f: \text{U}(N) \rightarrow \mathbb{R}$  is defined by

$$f(U) := \text{Tr}(HU\psi_0U^\dagger) = \langle\psi_0|U^\dagger HU|\psi_0\rangle. \quad (7)$$

To solve the above problem on the manifold  $U(N)$ , we will employ geometric tools and algorithms from the manifold optimization framework [21, 23]. In the main text that follows, we only briefly describe the geometric tools on  $U(N)$ . A detailed introduction to the geometry of the unitary manifold is provided in Section A.

To characterize the directions of infinitesimal motion on the manifold  $U(N)$ , we introduce the tangent space. For any  $U \in U(N)$ , the tangent space at  $U$  is given by

$$T_U := \{\Omega U : \Omega^\dagger = -\Omega\} = \mathfrak{u}(N)U, \quad (8)$$

where

$$\mathfrak{u}(N) := \{\Omega \in \mathbb{C}^{N \times N} : \Omega^\dagger = -\Omega\} \quad (9)$$

denotes the Lie algebra of  $U(N)$ , i.e., the real vector space of all  $N \times N$  skew-Hermitian matrices. Intuitively, the tangent space can be viewed as the tangent plane to the manifold at a given point (see Fig. 1).

For an unconstrained optimization problem, it is well known that the optimality condition is that the gradient vanishes. When the problem is restricted to a manifold, this condition becomes the vanishing of the Riemannian gradient (see Section A for more). Let  $\psi_U := U\psi_0U^\dagger$  denote the density operator corresponding to the output state of the circuit  $U$ . The *Riemannian gradient* of  $f$  at some  $U \in U(N)$  is given by

$$\text{grad } f(U) = [H, \psi_U]U \in T_U, \quad (10)$$

where  $[A, B] := AB - BA$ . For convenience, we denote the corresponding skew-Hermitian part by

$$\widetilde{\text{grad}}f(U) = [H, \psi_U] \in \mathfrak{u}(N). \quad (11)$$

When discussing the tangent space  $T_U = \mathfrak{u}(N)U$ , we often focus on  $\mathfrak{u}(N)$  itself and omit the right unitary  $U$ . [37, Theorem 3.2] has shown that  $\widetilde{\text{grad}}f(U^*) = 0$  if and only if  $U^* \in U(N)$  globally minimizes  $f(U)$  over  $U(N)$  with the minimum value 0, or globally maximizes it with the maximum value 1.

**Remark 1.** *Note that the above global optimality condition, resembling that of a convex function, is quite special. It holds only for Hamiltonians satisfying  $H = H^2$ . In general cases, it serves merely as a necessary condition for a local extremum.*

### III. GROVER-COMPATIBLE RIEMANNIAN GRADIENT ASCENT METHOD

In this section, we introduce the Grover-compatible Riemannian gradient ascent (RGA) method for problem Eq. (5). The term *gradient ascent* indicates that it is a typical first-order optimization algorithm. The term *Grover-compatible* means that each iteration is implemented using the diffusion and oracle operators (Eqs. (2) and (3)) from Grover's algorithm, making the

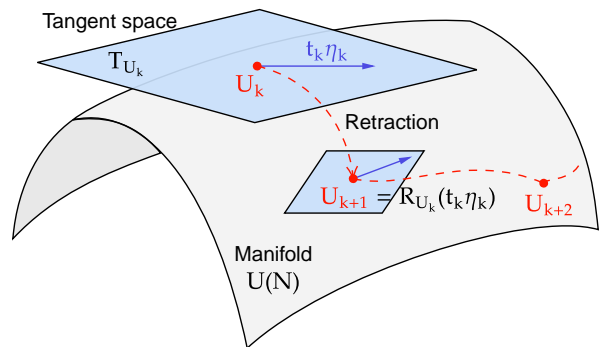


**Figure 1:** Schematic illustration of a manifold optimization iteration on the unitary manifold  $U(N)$ . Starting from the current point  $U_k$ , a tangent direction  $\eta_k \in T_{U_k}$  (e.g., the Riemannian gradient) is chosen in the tangent space. The retraction  $R_{U_k}$  then maps the scaled tangent vector  $t_k \eta_k$  back onto the manifold, producing the next iterate  $U_{k+1} = R_{U_k}(t_k \eta_k)$ .

method easy to realize on quantum hardware. This RGA method, originally proposed in the author's previous work [37], serves as a key foundation for the second-order method, the Grover-compatible Riemannian modified Newton method, developed in this work.

#### A. From Euclidean iterations to manifold iterations

Recall that in the classical Euclidean setting, to solve the optimization problem  $\max_{x \in \mathbb{R}^n} f(x)$ , one typically constructs a sequence  $\{x_k\} \subseteq \mathbb{R}^n$  from an initial iterate  $x_0 \in \mathbb{R}^n$  using the update rule

$$x_{k+1} = x_k + t_k \eta_k, \quad (12)$$

where  $\eta_k \in \mathbb{R}^n$  is a search direction (e.g., usual gradient  $\nabla f(x_k)$ ) and  $t_k > 0$  is a step size. To extend the update scheme Eq. (12) to manifolds, the search direction  $\eta_k$  is now chosen in the tangent space, and a mapping called *retraction* is used to map  $t_k \eta_k$  back to the manifold.

Specifically, to solve the manifold optimization problem  $\max_{U \in U(N)} f(U)$ , starting from an initial point  $U_0 \in U(N)$ , a sequence  $\{U_k\} \subseteq U(N)$  is generated via update rule (see Fig. 1 for a schematic illustration):

$$U_{k+1} = R_{U_k}(t_k \eta_k), \quad (13)$$

where  $\eta_k \in T_{U_k}$  is a tangent vector at the current point (e.g., Riemannian gradient  $\eta_k = \text{grad } f(U_k)$ ), and  $t_k > 0$  is still a step size. The mapping  $R_U : T_U \rightarrow U(N)$  is called a *retraction*, which enables movement along tangent directions while keeping iterates on the manifold. Formally, a retraction is a smooth mapping  $R_U : T_U \rightarrow U(N)$  such that the induced curve  $t \mapsto \gamma(t) := R_U(t\eta)$  satisfies

$$\gamma(0) = U, \quad \dot{\gamma}(0) = \eta, \quad \forall \eta \in T_U. \quad (14)$$

A natural example of a retraction on  $U(N)$  is the *Riemannian exponential map*, defined by

$$R_U^{\text{exp}}(\eta) = e^{\tilde{\eta}U}, \quad \tilde{\eta} := \eta U^\dagger \in \mathfrak{u}(N). \quad (15)$$

The induced curve then  $\gamma(t) = e^{t\tilde{\eta}U}$  satisfies  $\gamma(0) = U$  and  $\dot{\gamma}(0) = \tilde{\eta}U = \eta$ , verifying that  $R_U^{\text{exp}}$  is a valid retraction. Other examples are provided in Section A.

At this point, we can consider the simplest first-order optimization algorithm, i.e., the Riemannian gradient ascent method with the retraction  $R = R_U^{\text{exp}}$  defined in Eq. (15). Its update rule takes the form ( $k = 0, 1, \dots$ )

$$U_{k+1} = R_{U_k}^{\text{exp}}(t_k \text{grad } f(U_k)) = e^{t_k[H, \psi_k]} U_k, \quad (16)$$

where  $\psi_k := U_k \psi_0 U_k^\dagger$  denotes the intermediate quantum state after the  $k$ -th iteration. Setting the initial gate to  $U_0 = I$ , the resulting state after  $T$  iterations is

$$|\psi_T\rangle = e^{t_{T-1}[H, \psi_{T-1}]} \dots e^{t_1[H, \psi_1]} e^{t_0[H, \psi_0]} |\psi_0\rangle. \quad (17)$$

However, exactly implementing the newly introduced gate  $e^{t_k[H, \psi_k]}$  on quantum hardware is very challenging. Current works [28–31] address this issue by using stochastic subspace projected gradient. In these approaches, the Riemannian gradient  $[H, \psi_k]$  is projected onto a small number of randomly selected Pauli words, which form a basis of a random subspace in the tangent space  $\mathfrak{u}(N)$ ; a Trotter approximation [43] is then used as the retraction (see Eq. (A11) in Section A). However, such methods can only exploit partial information of the Riemannian gradient at each iteration. As we will soon see, for the Hamiltonian  $H = H^2$  arising in the Grover setting, there exists an exact implementation of the Riemannian gradient, rather than merely an approximate one.

## B. Grover-compatible retractions

The difficulty of implementing the gate  $e^{t_k[H, \psi_k]}$  in Eq. (16) suggests that the Riemannian exponential map  $R_U = R_U^{\text{exp}}$  in Eq. (15) may not be a practical choice of retraction. Note that the convergence guarantees of manifold optimization [21, 23] only require a retraction  $R_U$  to satisfy the first-order properties:  $\gamma(0) = U$ ,  $\dot{\gamma}(0) = \eta$  in Eq. (14); while its specific form is unrestricted. This motivates us to adopt another retraction that is easier to implement on quantum devices.

Throughout the remainder of the paper, let  $H = H^\dagger = H^2$  be an orthogonal projector on Hilbert space  $\mathcal{H}$  and  $M = \text{rank}(H)$ ; let  $|\psi_0\rangle \in \mathcal{H}$  be a unit vector and set  $\psi_0 = |\psi_0\rangle\langle\psi_0|$ . Assume that  $\langle\psi_0|H|\psi_0\rangle \notin \{0, 1\}$ . Define the Frobenius norm by  $\|A\|_F^2 = \langle A, A \rangle$ . We begin with an auxiliary lemma.

**Lemma 1** ([37, Lemma 3.2]). *Let  $\psi = |\psi\rangle\langle\psi|$  be any pure state and define  $q := \langle\psi|H|\psi\rangle$ . Define two skew-Hermitian operators by  $X := [H, \psi]$  and  $Y := i[H, X]$ . Then  $\|X\|_F = \|Y\|_F = \sqrt{2q(1-q)}$  and  $\langle X, Y \rangle = 0$ .*

The following Theorem 1 shows that if the circuit structure consists only of the diffusion and oracle operators defined in Eqs. (2) and (3), then the output states always remain in the Grover plane. More importantly, the corresponding Riemannian gradient also stays within a fixed two-dimensional subspace of the tangent space. Note that  $X_0$  and  $Y_0$  defined in Eq. (19) are orthogonal, as stated in Lemma 1.

**Theorem 1** (Invariant 2D gradient subspace [37, Theorem 3.3]). *Initialize the unitary by setting  $U_0 = I$ . For  $k = 0, 1, \dots$ , consider the update rule:*

$$V_k := \text{a finite product of the form } e^{i\theta H} \text{ and } e^{i\theta\psi_0}, \quad (18)$$

and define  $U_{k+1} := V_k U_k$ . Moreover, let  $\psi_k := |\psi_k\rangle\langle\psi_k|$ , where  $|\psi_k\rangle = U_k |\psi_0\rangle$ ; equivalently,  $|\psi_{k+1}\rangle = V_k |\psi_k\rangle$ . Define the scalars  $q_k := f(U_k) = \langle\psi_k|H|\psi_k\rangle \in [0, 1]$ , and the skew-Hermitian operators

$$X_0 := [H, \psi_0], \quad Y_0 := i[H, X_0]. \quad (19)$$

Then, for all  $k \geq 0$ , the following statements hold:

1. The state  $|\psi_k\rangle$  remains in the fixed 2-dimensional subspace (called Grover plane)

$$|\psi_k\rangle \in \mathcal{S} := \text{span}_{\mathbb{C}}\{|\psi_0\rangle, H|\psi_0\rangle\} \subseteq \mathcal{H}. \quad (20)$$

2. The skew-Hermitian part of Riemannian gradient,  $[H, \psi_k]$ , remains in the fixed 2-dimensional real subspace

$$[H, \psi_k] \in \mathcal{W} := \text{span}_{\mathbb{R}}\{X_0, Y_0\} \subseteq \mathfrak{u}(N), \quad (21)$$

$$\text{and } \|[H, \psi_k]\|_F = \sqrt{2q_k(1-q_k)}.$$

Theorem 1 provides an important insight: if the current gradient<sup>1</sup> lies in the 2-dimensional subspace  $\mathcal{W} \subseteq \mathfrak{u}(N)$  (when  $U_0 = I$ , the initial Riemannian gradient is simply  $X_0 \in \mathcal{W}$ ), then it suffices to consider a retraction that is well-defined only on  $\mathcal{W}$ , rather than on the full  $N^2 = 4^n$ -dimensional space  $\mathfrak{u}(N)^2$ . First, to ensure that it is a valid retraction, it must satisfy the standard first-order properties in Eq. (14). Second, to guarantee that the next Riemannian gradient remains in  $\mathcal{W}$ , its construction must involve only the form  $e^{i\theta H}$  and  $e^{i\theta\psi_0}$ . In this way, the whole procedure forms a closed loop. This naturally leads to the following definition.

**Definition 1.** *A mapping  $R_U$  is called a Grover-compatible retraction if for all  $U \in U(N)$  the following conditions hold:*

<sup>1</sup> In what follows, whenever there is no ambiguity, the term *gradient* also refers to the skew-Hermitian part of the Riemannian gradient.

<sup>2</sup> A typical contrast is the Trotter retraction defined in Eq. (A11) (see Section A).

1.  $R_U : \mathcal{WU} \rightarrow \text{U}(N)$  is a well-defined retraction restricted to the domain  $\mathcal{WU} \subseteq T_U = \mathfrak{u}(N)U$ ; that is, the induced curve  $\gamma(t) = R_U(t\eta)$  for  $t \geq 0$  satisfies

$$\gamma(0) = U, \quad \dot{\gamma}(0) = \eta, \quad \forall \eta \in \mathcal{WU}. \quad (22)$$

2.  $R_U$  admits the form  $R_U(\eta) = V(\eta)U$ , where  $V(\eta)$  is a finite product of the form  $e^{i\theta H}$  and  $e^{i\theta\psi_0}$ .

In fact, retractions satisfying the above definition are easy to construct, and their forms may vary. Here we introduce a 5-factor retraction in Example 1. According to the number  $K$  of factors of the form  $e^{i\theta H}$  and  $e^{i\theta\psi_0}$  it contains, we refer to it as a  $K$ -factor retraction. More examples, such as 6-factor and 8-factor retractions, can be found in [37, Proposition 3.5].

**Example 1** (5-factor retraction). For any  $U \in \text{U}(N)$  and  $\eta \in \mathcal{WU}$ , write the skew-Hermitian part  $\tilde{\eta} := \eta U^\dagger \in \mathcal{W}$  in the form  $\tilde{\eta} = xX_0 + yY_0$  for unique coefficients  $(x, y) \in \mathbb{R}^2$ . Let  $A := \text{atan2}(y, x)$  and  $R := \sqrt{x^2 + y^2}$ , which correspond to the argument and modulus of the complex number  $x + iy$ , and define

$$a_1 := A + \frac{\pi}{2}, \quad a_2 := A - \frac{\pi}{2}, \quad b_1 := -\frac{R}{2}, \quad b_2 := \frac{R}{2}. \quad (23)$$

The 5-factor retraction is defined by

$$R_U^{(5)}(\eta) := e^{ia_1 H} e^{ib_1 \psi_0} e^{i(a_2 - a_1)H} e^{ib_2 \psi_0} e^{-ia_2 H} U. \quad (24)$$

Since  $a_2 - a_1 = -\pi$ , the middle  $H$ -exponential simplifies to  $e^{-i\pi H}$ . For  $t \geq 0$ , the associated curve is given by

$$\gamma(t) = \underbrace{e^{ia_1 H} e^{ib_1 \psi_0} e^{-i\pi H} e^{ib_2 \psi_0} e^{-ia_2 H}}_{\text{newly added gates } V(t;x,y):=} U. \quad (25)$$

It can be verified that  $\gamma(0) = U$  and  $\dot{\gamma}(0) = \eta \in \mathcal{WU}$ .

Indeed, the Grover-compatible retractions  $R_U : \mathcal{WU} \simeq \mathbb{R}^2 \rightarrow \text{U}(N)$  admit the following general abstract form:

$$R_U(t\eta) = \underbrace{\left( \prod_{\ell=1}^K e^{i\theta_\ell^{(1)}(t;x,y)H} e^{i\theta_\ell^{(2)}(t;x,y)\psi_0} \right)}_{\text{newly added gates } V(t;x,y):=} U, \quad (26)$$

for  $\tilde{\eta} := \eta U^\dagger = xX_0 + yY_0 \in \mathcal{W}$ . The order of  $H$ - and  $\psi_0$ -exponentials does not matter. Now, we provide the Riemannian gradient ascent (RGA) method employing Grover-compatible retractions in Algorithm 1.

[37, Theorem 4.6] provides explicit results on the convergence and complexity of Algorithm 1. Suppose we run Algorithm 1 with the 5-factor retraction in Eq. (24), and choose a fixed step size  $t_k = 1/L_{\text{Rie}}$ , where  $L_{\text{Rie}} := 2 + N/\sqrt{2M(N-M)} \in \mathcal{O}(\sqrt{N/M})$ . Then, for any  $0 < \varepsilon \leq q_0$ , the iterates satisfy  $1 - q_T \leq \varepsilon$  within at most  $T = \lceil 6L_{\text{Rie}} \log(1/\varepsilon) \rceil$  iterations. In summary, we establish an iteration complexity of  $\mathcal{O}(\sqrt{N/M} \log(1/\varepsilon))$  to reach an  $\varepsilon$ -global maximizer, which is consistent with Grover's quadratic speedup. The term  $\log(1/\varepsilon)$  indicates that the method converges linearly with respect to the accuracy  $\varepsilon$ .

---

### Algorithm 1: Grover-compatible Riemannian gradient ascent (RGA) method

---

**Input:** Choose a Grover-compatible retraction  $R$  in Definition 1 with formula Eq. (26), initial point  $U_0 = I$ , and tolerance  $\varepsilon$ .

- 1 Set  $k := 0$ ,  $q_0 := M/N$ ;
  - 2 **while**  $\|[H, \psi_k]\| > \varepsilon$  **do**
  - 3     Decompose  $[H, \psi_k] = x_k X_0 + y_k Y_0$  to find  $(x_k, y_k) \in \mathbb{R}^2$ ;
  - 4     Choose a step size  $t_k > 0$ ;
  - 5     Update  $U_{k+1} := V(t_k; x_k, y_k)U_k$  by Eq. (26);
  - 6     Update  $|\psi_{k+1}\rangle := V(t_k; x_k, y_k)|\psi_k\rangle$ ;
  - 7     Compute new cost value  $q_{k+1} := \langle \psi_{k+1} | H | \psi_{k+1} \rangle$ ;
  - 8     Compute  $\|[H, \psi_{k+1}]\|_F := \sqrt{2q_{k+1}(1 - q_{k+1})}$ ;
  - 9     Set  $k := k + 1$ ;
- 

**Remark 2.** Note that as long as the initial state  $|\psi_0\rangle$  is the uniform state, Algorithm 1 is guaranteed to converge to the desired target state  $|\psi^*\rangle$  defined in Eq. (4). Recall that  $|\psi^*\rangle = (1/\sqrt{q_0})H|\psi_0\rangle$ . For any  $|\psi_k\rangle \in \mathcal{S} = \text{span}_{\mathbb{C}}\{|\psi_0\rangle, H|\psi_0\rangle\}$ , the cost value satisfies  $q_k = \langle \psi_k | H | \psi_k \rangle = |\langle \psi_k | \psi^* \rangle|^2$ . Therefore, when  $q_k \rightarrow 1$ , the states  $|\psi_k\rangle$  and  $|\psi^*\rangle$  differ only by a global phase.

### C. Classical simulability of Algorithm 1

Algorithm 1 does not need to be executed directly on a quantum device. As shown in Theorem 2, the procedure is classically simulable. Intuitively, the entire evolution of Algorithm 1 takes place within a two-dimensional subspace. We choose  $u := H|\psi_0\rangle$  and  $v := (I - H)|\psi_0\rangle$  as a basis for the Grover plane. It therefore suffices to represent the state  $|\psi_k\rangle$  and the gradient  $[H, \psi_k]$  in this basis. The detailed proof can be found in [37, Theorem 3.8]. In practice, the gate angles can be computed in advance on a classical computer, after which the resulting circuit is executed on quantum hardware.

**Theorem 2** (Classical simulability of Algorithm 1 [37, Theorem 3.8]). *Consider the iterative process in Algorithm 1. With the initial triplet  $(x_0, y_0, q_0) := (1, 0, q_0)$  and the  $2 \times 2$  matrix  $\Psi_0 = \begin{bmatrix} q_0 & 1 - q_0 \\ q_0 & 1 - q_0 \end{bmatrix}$ , there exists an explicit, classically computable process*

$$F_{\text{RGA}} : (x_k, y_k, q_k; t_k) \mapsto (x_{k+1}, y_{k+1}, q_{k+1}), \quad (27)$$

described as follows. Initialize  $\alpha_0 = \beta_0 = 1$ , and  $z_0 = \alpha_0 \beta_0$ . For each  $k = 0, 1, \dots$ ,

1. For the additional update gates  $V(t_k; x_k, y_k)$  in Eq. (26), define the corresponding  $2 \times 2$  matrix

$$M_k := \prod_{\ell=1}^K E_H(\theta_\ell^{(1)}(t_k; x_k, y_k)) E_{\psi_0}(\theta_\ell^{(2)}(t_k; x_k, y_k)),$$

where  $E_H(\theta) = \begin{bmatrix} e^{i\theta} & 0 \\ 0 & 1 \end{bmatrix}$ ,  $E_{\psi_0}(\theta) = I_2 + (e^{i\theta} - 1)\Psi_0$ .

2. Update  $\begin{pmatrix} \alpha_{k+1} \\ \beta_{k+1} \end{pmatrix} = M_k \begin{pmatrix} \alpha_k \\ \beta_k \end{pmatrix}$ , and let  $q_{k+1} = q_0 |\alpha_{k+1}|^2$ ,  $z_{k+1} = \alpha_{k+1} \bar{\beta}_{k+1}$ ,  $x_{k+1} = \Re(z_{k+1})$ ,  $y_{k+1} = \Im(z_{k+1})$ .
3. Set  $k \leftarrow k + 1$  and return to step 1.

As we will see later, the Riemannian Newton method proposed in this work is also classically simulable and can be obtained with modifications based on Theorem 2.

#### IV. GROVER-COMPATIBLE RIEMANNIAN MODIFIED NEWTON METHOD

In the classical Euclidean setting, consider the optimization problem  $\max_{x \in \mathbb{R}^n} f(x)$ . A prototypical second-order algorithm is the Newton method [44–46], which updates via the Hessian matrix:

$$x_{k+1} = x_k + d_k, \quad d_k = -[\nabla^2 f(x_k)]^{-1} \nabla f(x_k), \quad (28)$$

where  $d_k$  denotes the Newton direction. Under standard regularity conditions, the method exhibits quadratic convergence in a neighborhood of the solution. The Newton method has also been extended to optimization on manifolds [21, 38, 47], while preserving the same quadratic convergence rate with respect to the accuracy  $\varepsilon$ .

In this section, building on the first-order framework developed in the previous section, we will replace the Riemannian gradient direction with the Riemannian Newton direction, thereby obtaining a Grover-compatible Riemannian Newton method. This modification is expected to improve the complexity from  $\mathcal{O}(\sqrt{N/M} \log(1/\varepsilon))$  to  $\mathcal{O}(\sqrt{N/M} \log \log(1/\varepsilon))$ .

##### A. Riemannian Hessian

For  $f : \mathbb{R}^n \rightarrow \mathbb{R}$ , the Hessian matrix  $\nabla^2 f(x)$  at a point  $x$  captures the second-order information of  $f$ . It is an  $n \times n$  symmetric matrix and can be viewed as a self-adjoint linear operator on  $\mathbb{R}^n$ . By analogy, when  $f$  is defined on a manifold, the Riemannian Hessian (operator) can be regarded as a self-adjoint linear operator acting on the tangent space. For the cost function defined in Eq. (7), we have the following lemma.

**Lemma 2** ([31, Proposition 1]). *For the cost function  $f : \mathbf{U}(N) \rightarrow \mathbb{R}$  defined by  $f(U) = \text{Tr}(HU\psi_0U^\dagger)$ , the Riemannian Hessian of  $f$  at  $U \in \mathbf{U}(N)$  is the self-adjoint linear map  $\text{Hess } f(U) : T_U \rightarrow T_U$ ,*

$$\text{Hess } f(U)[\Omega U] = \frac{1}{2}([H, [\Omega, \psi_U]] + [[H, \Omega], \psi_U])U, \quad (29)$$

where  $\psi_U = U\psi_0U^\dagger$  and  $T_U = \mathbf{u}(N)U$ . Identifying  $T_U \simeq \mathbf{u}(N)$  yields  $\widetilde{\text{Hess}}f(U) : \mathbf{u}(N) \rightarrow \mathbf{u}(N)$ ,

$$\widetilde{\text{Hess}}f(U)[\Omega] = \frac{1}{2}([H, [\Omega, \psi_U]] + [[H, \Omega], \psi_U]), \quad (30)$$

which is self-adjoint on  $\mathbf{u}(N)$ .

The self-adjointness means that  $\langle \Xi, \widetilde{\text{Hess}}f(U)[\Omega] \rangle = \langle \widetilde{\text{Hess}}f(U)[\Xi], \Omega \rangle$  for any  $\Omega, \Xi \in \mathbf{u}(N)$ . A derivation of this Hessian expression can be found in [31, Proposition 1]. An equivalent definition is based on the second-order Taylor expansion on the manifold:

$$\begin{aligned} f(R_U(t\eta)) & \\ &= f(U) + t \langle \text{grad } f(U), \eta \rangle + \frac{t^2}{2} \langle \eta, \text{Hess } f(U)[\eta] \rangle + \mathcal{O}(t^3), \end{aligned} \quad (31)$$

where  $R_U$  is a retraction and  $\eta \in T_U$ . In Section A, we verify that Eq. (29) ensures the above expansion holds.

In the classical Euclidean setting, the Newton direction  $d_k$  is defined as the solution to the Newton equation:

$$\nabla^2 f(x_k) d_k = -\nabla f(x_k). \quad (33)$$

By analogy, the Riemannian Newton direction  $\Omega_k^N U_k \in T_{U_k}$  is defined as the solution to the Riemannian Newton equation:  $\text{Hess } f(U_k)[\Omega_k^N U_k] = -\text{grad } f(U_k)$ , i.e.,

$$\widetilde{\text{Hess}}f(U_k)[\Omega_k^N] = -\widetilde{\text{grad}}f(U_k). \quad (34)$$

Solving these equations is generally challenging. In [31], Pauli words are used as a basis of  $\mathbf{u}(N)$  to convert the above operator equation into a matrix equation. However, this approach is computationally expensive.

In contrast, in the Grover setting, where the Hamiltonian satisfies  $H = H^2$ , a remarkable relationship arises: the Riemannian gradient is always an eigenvector of the Riemannian Hessian. Consequently, the Newton equation admits an explicit solution. This result is formalized in the following theorem, with the proof provided in Section B.

**Theorem 3.** *Let  $H = H^\dagger = H^2$  be an orthogonal projector, and let  $\psi = |\psi\rangle\langle\psi|$  be an arbitrary pure state. Define  $q := \text{Tr}(H\psi) \in [0, 1]$  and  $g := [H, \psi]$ . Consider the map  $L(\Omega) := \frac{1}{2}([H, [\Omega, \psi]] + [[H, \Omega], \psi])$ . Then  $L(g) = (1 - 2q)g$ .*

Note that the above result holds only under the condition  $H = H^2$ , and does not hold in general.

##### B. Grover-compatible Riemannian modified Newton method

In this subsection, we are now ready to present a Riemannian Newton method for problem Eq. (5), which is

both Grover-compatible and classically simulable, similar to Algorithm 1. Let  $q_k = f(U_k)$ , and define

$$\mathbf{g}_k := \widetilde{\text{grad}}f(U_k) \neq 0, \quad \mathbf{H}_k := \widetilde{\text{Hess}}f(U_k). \quad (35)$$

Then Theorem 3 shows that

$$\mathbf{H}_k[\mathbf{g}_k] = \lambda_k \mathbf{g}_k, \quad \lambda_k := 1 - 2q_k. \quad (36)$$

Since  $q_k \in [0, 1]$ , the eigenvalue  $\lambda_k$  lies in the interval  $[-1, 1]$ . The original Newton equation  $\mathbf{H}_k[\Omega_k^N] = -\mathbf{g}_k$  in Eq. (34) therefore admits the explicit solution

$$\Omega_k^N = \frac{1}{-\lambda_k} \mathbf{g}_k \in \mathcal{W}, \quad (37)$$

whenever  $q_k \neq \frac{1}{2}$ . (Recall that  $\mathcal{W} := \text{span}_{\mathbb{R}}\{X_0, Y_0\} \subseteq \mathfrak{u}(N)$  as defined in Theorem 1.) The corresponding standard Newton update is then given by  $U_{k+1} = R_{U_k}(\Omega_k^N)$  with unit step size  $t_k = 1$ .

**Remark 3.** *Since the Riemannian gradient is always an eigenvector of the Riemannian Hessian, the Newton direction is collinear with the gradient. Then, the Newton method can be viewed as a scaled gradient method.*

However, the standard Newton method converges only when the initial point  $U_0$  is sufficiently close to the solution. To improve numerical stability, we therefore employ a modified Newton method [46]. Specifically, we introduce a parameter  $\mu_k \geq 0$  to modify the Hessian operator and solve the modified Newton equation

$$(\mathbf{H}_k - \mu_k \mathbf{I})[\Omega_k^N] = -\mathbf{g}_k, \quad (38)$$

where  $\mathbf{I}$  denotes the identity operator on the tangent space  $\mathfrak{u}(N)$ . By Theorem 3, this equation also admits a solution, namely the modified Newton direction

$$\Omega_k^N = \gamma_k \mathbf{g}_k \in \mathcal{W}, \quad \gamma_k := \frac{1}{\mu_k - \lambda_k}, \quad (39)$$

whenever  $\mu_k \neq \lambda_k$ . If we set  $\mu_k > \lambda_k$ , then

$$\langle \Omega_k^N, \mathbf{g}_k \rangle = \gamma_k \|\mathbf{g}_k\|^2 = \gamma_k 2q_k(1 - q_k) > 0. \quad (40)$$

Hence, the modified Newton direction is an ascent direction, and there always exists a step size  $t_k > 0$  along this direction that increases the cost value. The parameter  $\mu_k$  is determined according to the following two cases:

1. If  $q_k > 0.5$ , then  $\lambda_k < 0$ . In this case, the Hessian operator is already negative along the gradient direction. We therefore set  $\mu_k = 0$ , which yields  $\gamma_k = \frac{1}{-\lambda_k}$  like Eq. (37).
2. If  $q_k \leq 0.5$ , then  $\lambda_k \geq 0$ . In this case, the Hessian operator is positive along the gradient direction, and the unmodified Newton step would point toward a descent direction. To avoid this, we set  $\mu_k = \lambda_k + \delta$  with  $\delta > 0$ , which yields  $\gamma_k = \frac{1}{\delta}$ .

---

**Algorithm 2:** Grover-compatible Riemannian modified Newton (RMN) method

---

**Input:** Choose a Grover-compatible retraction  $R$  in Definition 1 with formula Eq. (26), initial point  $U_0 = I$ , damping  $\delta = 10^{-3}$ , Armijo parameters  $c = 10^{-4}$ ,  $\rho = \frac{1}{2}$ , and tolerance  $\varepsilon$ .

- 1 Set  $k := 0$ ,  $q_0 := M/N$ , and initial squared gradient norm  $G_0 := 2q_0(1 - q_0)$ ;
  - 2 **while**  $\sqrt{G_k} > \varepsilon$  **do**
  - 3   Decompose  $[H, \psi_k] = x_k X_0 + y_k Y_0$  to find  $(x_k, y_k) \in \mathbb{R}^2$ ;
  - 4   Set modified Newton scaling  $\gamma_k := \frac{1}{\max(\delta, 2q_k - 1)}$ ;
  - 5   Set step size  $t := 1$ ;
  - 6   **repeat**
  - 7     Set  $|\psi_{\text{trial}}\rangle := V(t\gamma_k; x_k, y_k)|\psi_k\rangle$  by Eq. (26);
  - 8     Compute  $q_{\text{trial}} := \langle \psi_{\text{trial}} | H | \psi_{\text{trial}} \rangle$ ;
  - 9     **if**  $q_{\text{trial}} < q_k + c t \gamma_k G_k$  **then**
  - 10      Set  $t := \rho t$ ;
  - 11   **until**  $q_{\text{trial}} \geq q_k + c t \gamma_k G_k$ ;
  - 12   Update  $U_{k+1} := V(t\gamma_k; x_k, y_k)U_k$ ;
  - 13   Update  $|\psi_{k+1}\rangle := |\psi_{\text{trial}}\rangle$ ;
  - 14   Update  $q_{k+1} := q_{\text{trial}}$ ;
  - 15   Update  $G_{k+1} := 2q_{k+1}(1 - q_{k+1})$ ;
  - 16   Set  $k := k + 1$ ;
- 

Combining the two cases above, we set the scaling factor

$$\gamma_k = \frac{1}{\max(\delta, 2q_k - 1)} \quad (41)$$

where  $\delta > 0$  is a small constant, typically chosen in the range  $10^{-3} \sim 10^{-6}$ .

After ensuring that the Newton direction  $\Omega_k^N$  is an ascent direction, we further employ an Armijo backtracking line search; see [46, Algorithm 3.2]. Specifically, we seek the smallest integer  $m \geq 0$  such that  $t_k = \rho^m$  satisfies

$$f(R_{U_k}(t_k \Omega_k^N)) \geq f(U_k) + c t_k \langle \Omega_k^N, \mathbf{g}_k \rangle, \quad (42)$$

where  $\rho = 0.5$  and  $c = 10^{-4}$ . Note that  $\langle \Omega_k^N, \mathbf{g}_k \rangle > 0$ , which guarantees that the above procedure terminates after finitely many iterations; see [46, Lemma 3.1]. Consequently, the cost value increases monotonically. Finally, a complete description of the proposed algorithm is given in Algorithm 2.

This modified Newton method with line search ensures convergence from any initial point (i.e., it enjoys the global convergence property of first-order gradient methods), while achieving quadratic convergence once the iterate is sufficiently close to the solution. Intuitively, during the early iterations, Algorithm 2 behaves similarly to Algorithm 1. When the iterate is sufficiently close to the solution (so that  $q_k > 0.5$  and no direction modification is required), the Armijo condition is always satisfied with  $t_k = 1$ ; see [46, Theorem 3.6 & 3.8]. Consequently, Algorithm 2 reduces to the standard Newton method.

### C. Classical simulability of Algorithm 2

Compared with the gradient ascent method in Algorithm 1, the modified Newton method in Algorithm 2 differs only by the introduction of a scaling factor  $\gamma_k$  and a line-search procedure. Building on the classical simulability of Algorithm 1 established in Theorem 2, we can directly derive a classically simulable version of Algorithm 2, as stated in the following theorem. All operations reduce to computations with  $2 \times 2$  matrices.

**Theorem 4** (Classical simulability of Algorithm 2). *Consider the iterative process in Algorithm 2. With the initial triplet  $(x_0, y_0, q_0) := (1, 0, q_0)$  and the  $2 \times 2$  matrix  $\Psi_0 = \begin{bmatrix} q_0 & 1 - q_0 \\ q_0 & 1 - q_0 \end{bmatrix}$ , there exists an explicit, classically computable process*

$$F_{\text{RMN}} : (x_k, y_k, q_k) \mapsto (x_{k+1}, y_{k+1}, q_{k+1}), \quad (43)$$

described as follows. Initialize  $G_0 = 2q_0(1 - q_0)$ ,  $\alpha_0 = \beta_0 = 1$ , and  $z_0 = \alpha_0 \bar{\beta}_0$ . For each  $k = 0, 1, \dots$ ,

1. Set modified scaling  $\gamma_k := \frac{1}{\max(\delta, 2q_k - 1)}$ .
2. For the trial step  $t$ , and additional update gates  $V(t\gamma_k; x_k, y_k)$  in Eq. (26), define the corresponding  $2 \times 2$  matrix

$$M_k(t) := \prod_{\ell=1}^K E_H(\theta_\ell^{(1)}(t\gamma_k; x_k, y_k)) E_{\psi_0}(\theta_\ell^{(2)}(t\gamma_k; x_k, y_k)),$$

$$\text{where } E_H(\theta) = \begin{bmatrix} e^{i\theta} & 0 \\ 0 & 1 \end{bmatrix}, E_{\psi_0}(\theta) = I_2 + (e^{i\theta} - 1)\Psi_0.$$

3. For the trial step  $t$ , define  $\begin{pmatrix} \alpha_k^{\text{temp}}(t) \\ \beta_k^{\text{temp}}(t) \end{pmatrix} := M_k(t) \begin{pmatrix} \alpha_k \\ \beta_k \end{pmatrix}$ , and  $q_k^{\text{temp}}(t) := q_0 |\alpha_k^{\text{temp}}(t)|^2$ .
4. Let  $m_k \geq 0$  be the smallest nonnegative integer such that the Armijo condition

$$q_k^{\text{temp}}(\rho^{m_k}) \geq q_k + c \rho^{m_k} \gamma_k G_k \quad (44)$$

holds, and set  $t_k := \rho^{m_k}$ .

5. Update  $\begin{pmatrix} \alpha_{k+1} \\ \beta_{k+1} \end{pmatrix} = M_k(t_k) \begin{pmatrix} \alpha_k \\ \beta_k \end{pmatrix}$ , and let  $q_{k+1} = q_0 |\alpha_{k+1}|^2$ ,  $G_{k+1} = 2q_{k+1}(1 - q_{k+1})$ ,  $z_{k+1} = \alpha_{k+1} \bar{\beta}_{k+1}$ ,  $x_{k+1} = \Re(z_{k+1})$ ,  $y_{k+1} = \Im(z_{k+1})$ .
6. Set  $k \leftarrow k + 1$  and return to step 1.

## V. NUMERICAL EXPERIMENTS

In this section, we compare the following methods via numerical simulations:

- the Grover-compatible Riemannian gradient ascent (**RGA**) method (Algorithm 1) [37], and
- the proposed Grover-compatible Riemannian modified Newton (**RMN**) method (Algorithm 2).

All experiments are implemented in the NumPy package and conducted on a MacBook Pro (2021) with an Apple M1 Pro processor and 16 GB of memory.

Consider an unstructured search problem of size  $N = 2^n$  for an  $n$ -qubit system, with a single marked item ( $M = 1$ ). We always use 5-factor retraction defined in Example 1. The initial state  $|\psi_0\rangle$  is the uniform superposition. The progress of the algorithms is measured by the cost value  $q_k = f(U_k) = \text{Tr}(H\psi_k)$ , which represents the success probability of identifying the marked item and should converge to 1 under RGA and RMN. Given  $\varepsilon > 0$  (typically  $10^{-10}$ ), the algorithms terminate when  $|1 - q_k| < \varepsilon$ .

*a. Correctness of classical simulability.* We first examine whether the classical procedures described in Theorems 2 and 4 can faithfully simulate the quantum implementations of Algorithms 1 and 2. To this end, we set  $n = 4$  qubits. At each iteration, we evaluate three quantities: the cost value  $q_k$ , and the coefficients  $x_k, y_k$ . Recall that  $x_k$  and  $y_k$  are the expansion coefficients of the Riemannian gradient  $[H, \psi_k]$  on the two-dimensional subspace  $\mathcal{W}$  with respect to the basis  $\{X_0, Y_0\}$ .

Fig. 2 reports the absolute errors of these three quantities for RGA ((a)–(c)) and RMN ((d)–(f)), with and without classical simulation. Here, “without classical simulation” refers to a direct NumPy implementation using explicit  $N \times N$  full matrix operations, following Algorithms 1 and 2 in a brute-force manner. The results show that the classical simulation accurately reproduces the true iterations up to machine precision ( $10^{-16}$ ). Therefore, all subsequent experiments are conducted under classical simulation.

*b. Comparison of convergence rates.* As a first-order optimization method, RGA is shown to achieve asymptotic linear convergence with respect to the error [37]. Let the function value error be denoted as  $\delta_k := |1 - q_k|$ . Then, there exist an integer  $k_1$  and a contraction factor  $\rho \in (0, 1)$  such that  $\delta_{k+1} \leq \rho \delta_k, \forall k \geq k_1$ . In contrast, the proposed RMN is a second-order method. RMN achieves local quadratic convergence: there exist an integer  $k_2$  and a constant  $C > 0$  such that  $\delta_{k+1} \leq C \delta_k^2, \forall k \geq k_2$ .

It is well known that quadratic convergence is significantly faster than linear convergence. For each case, we run both RGA (with fixed step size 0.5) and RMN. Fig. 3 shows the results on a log scale, including the gradient norm ((a)–(c)) and the function value error ((d)–(f)). The results show that RGA decreases linearly with respect to the iteration count. In contrast, RMN exhibits quadratic convergence and reaches a high-accuracy solution within only a few iterations. This behavior is evident in both the gradient norm and the function value error. For example, in (d), RMN reduces the error from  $10^{-2}$  to  $10^{-4}$ , and then to  $10^{-8}$  in just two iterations.

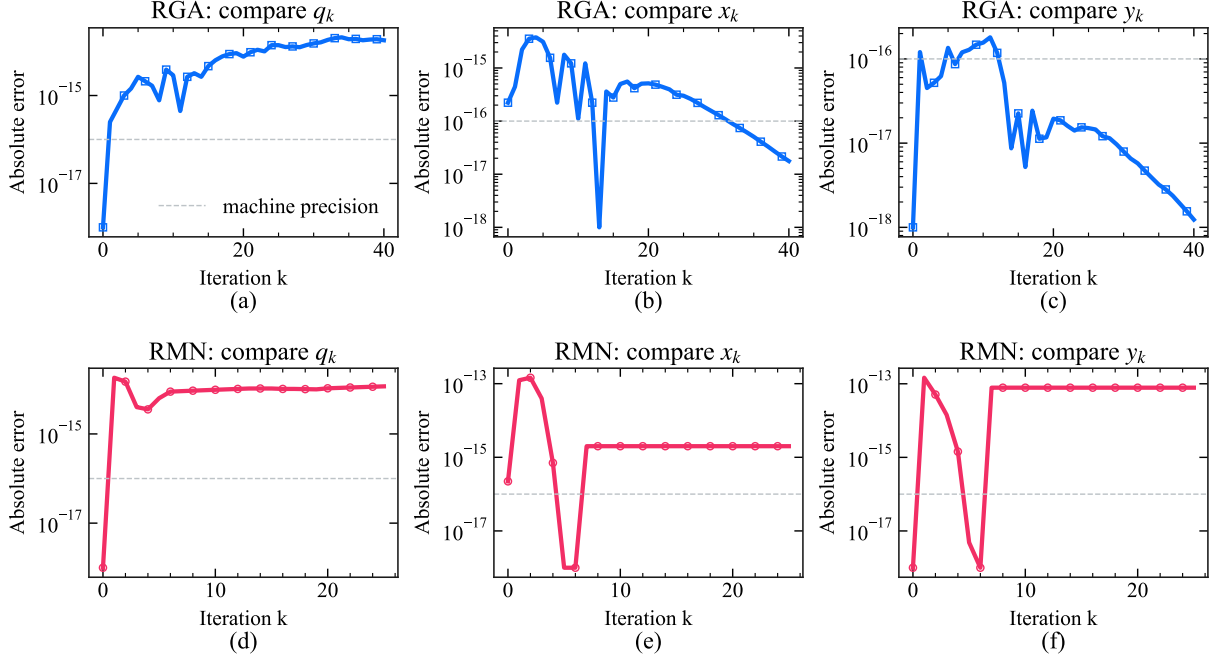


**Figure 2:** Absolute errors of the cost value  $q_k$  and expansion coefficients  $x_k, y_k$  between the classical simulation and the explicit full matrix implementation. (a)–(c) display the results for RGA, and (d)–(f) for RMN. All errors remain around machine precision ( $10^{-16}$ ), verifying that the classical procedures accurately simulate the algorithms.

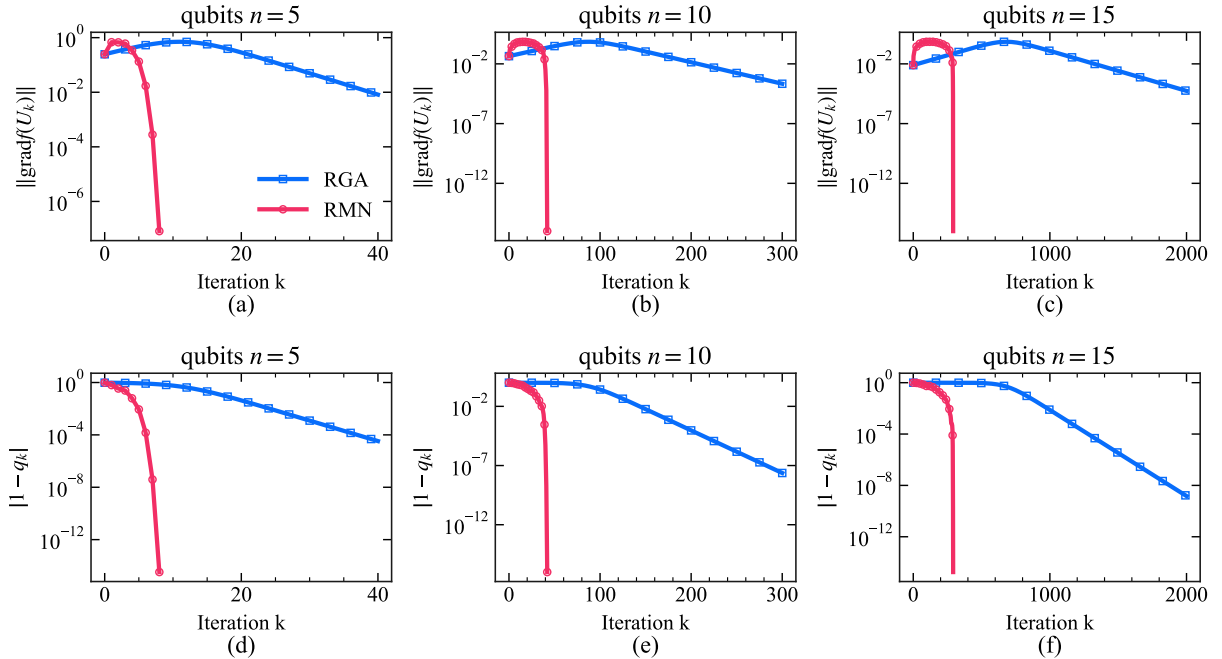


**Figure 3:** Convergence comparison between the RGA and RMN methods for problem sizes of  $n = 5, 10,$  and  $15$  qubits. (a)–(c) illustrate the gradient norm, and (d)–(f) show the function value error. The results demonstrate the linear convergence of RGA and the significantly faster, quadratic convergence of RMN.

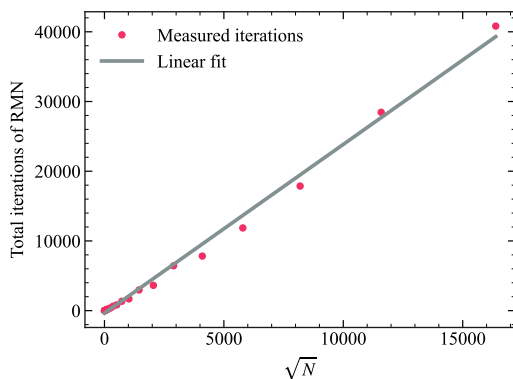


**Figure 4:** Iteration complexity of RMN versus the square root of the problem size. For a fixed tolerance  $\varepsilon$  and varying qubit counts  $n \in [2, 28]$  ( $N = 2^n$ ), the required iterations for RMN scale linearly with  $\sqrt{N}$ . This confirms that the second-order RMN method successfully retains the  $\mathcal{O}(\sqrt{N})$  quantum speedup.

*c. Scaling with problem size.* RGA is shown in [37] to have complexity  $\mathcal{O}(\sqrt{N/M} \log(1/\varepsilon))$ . Fixing the accuracy  $\varepsilon$  and setting  $M = 1$ , this reduces to the well-known quadratic speedup  $\mathcal{O}(\sqrt{N})$ , i.e., the iteration count grows linearly with  $\sqrt{N}$ . The proposed RMN is a second-order optimization method, whose improvement targets the dependence on the accuracy  $\varepsilon$  rather than on the problem size  $N^3$ . It is therefore expected to retain the same scaling  $\mathcal{O}(\sqrt{N})$  with respect to the problem size. However, due to its quadratic convergence, the overall complexity improves to  $\mathcal{O}(\sqrt{N/M} \log \log(1/\varepsilon))$ .

Next, we investigate the dependence of RMN on the problem size  $N$ . We fix  $\varepsilon = 10^{-6}$  and vary the number of qubits from  $n = 2$  to  $n = 28$ , corresponding to  $\sqrt{N}$  ranging from 2 to  $\sqrt{2^{28}} = 16384$ . Fig. 4 shows a clear linear relationship: the number of iterations of RMN to reach the prescribed accuracy scales proportionally to  $\sqrt{N}$ .

## VI. DISCUSSION

In this work, we develop a deeper understanding of the quantum search problem through the lens of the manifold optimization framework by introducing the Grover-compatible Riemannian modified Newton (RMN) method. While the previous first-order Riemannian gradient ascent (RGA) method [37] successfully recasts quantum search as a maximization problem on the unitary group and achieves  $\mathcal{O}(\sqrt{N} \log(1/\varepsilon))$  query complexity, it is limited to a linear convergence rate with respect to the target accuracy  $\varepsilon$ . By incorporating second-order geometric information, we overcome this limitation.

The cornerstone of our RMN method is the theoretical observation that, for projector Hamiltonians  $H = H^2$ , the Riemannian gradient is an eigenvector of the corresponding Riemannian Hessian. This property eliminates the need for costly Hessian inversion, reducing the Newton update to a scaled gradient step. Consequently, our RMN method can achieve a quadratic convergence rate, driving the total complexity down to  $\mathcal{O}(\sqrt{N} \log \log(1/\varepsilon))$  without incurring additional overhead per iteration. Furthermore, we demonstrate that the classical simulability of the parameter update process is also preserved, allowing for the efficient precomputation of gate angles prior to execution on quantum hardware.

Our results suggest several promising directions for future research. The exact collinearity of the Riemannian gradient and the Newton direction established in our framework (i.e., Theorem 3) relies strictly on the projective nature of the Grover Hamiltonian ( $H = H^2$ ). Therefore, extending this second-order geometric property to more general quantum tasks presents a compelling theoretical challenge. On the other hand, for broader quantum applications such as ground-state preparation for generic molecular Hamiltonians [48, 49], implementing exact Newton or gradient steps may be intractable on quantum computers. In such settings, it is of interest to investigate whether similar invariant gradient subspaces (as in Theorem 1) can be identified to reduce the effective problem dimensionality. Furthermore, the application of Riemannian quasi-Newton methods [50], particularly Riemannian BFGS [51], could offer a viable pathway to achieving superlinear convergence without the need for explicit Hessian evaluations, enabling accelerations across a wider spectrum of Hamiltonians.

Beyond those theoretical generalizations, future work can evaluate the resilience of the RMN method under realistic hardware noise, as high-precision algorithms may be sensitive to gate infidelities and decoherence in NISQ devices. Finally, integrating this manifold optimization framework with quantum error mitigation techniques may be essential to stabilize its quadratic convergence for practical implementations.

## ACKNOWLEDGMENTS

This work was supported by the National Natural Science Foundation of China under the grant numbers 12501419, 12331010 and 12288101, the National Key R&D Program of China under the grant number 2024YFA1012901, the Quantum Science and Technology-National Science and Technology Major Project via Project 2024ZD0301900, and the Fundamental Research Funds for the Central Universities, Peking University.

<sup>3</sup> Optimization literature typically fixes the problem size and studies how to achieve higher accuracy with fewer iterations.

## DATA AVAILABILITY

The source code of the numerical experiments is publicly available [52].

### Appendix A: Geometric tools on $U(N)$

The set of  $N \times N$  unitary matrices,

$$U(N) = \{U \in \mathbb{C}^{N \times N} \mid U^\dagger U = I\}, \quad (\text{A1})$$

forms a Riemannian manifold, despite being a subset of a Euclidean space. As a result, optimization over  $U(N)$  requires geometric tools tailored to the manifold structure. This appendix briefly reviews the basic ingredients for optimization on  $U(N)$ , including tangent spaces, Riemannian gradients, retractions, and Riemannian Hessians. For a comprehensive treatment, see [21, 23].

#### 1. Tangent space

Geometrically, the *tangent space* provides a local linear approximation of the manifold at a given point, analogous to a tangent plane to a two-dimensional sphere (see Fig. 5). From an optimization perspective, it consists of all feasible directions (i.e., tangent vectors) along curves on the manifold. This structure can also be characterized algebraically.

Fix a point  $U \in U(N)$ , and consider a smooth curve  $t \mapsto U(t) \in U(N)$  with  $U(0) = U$ . Differentiating the unitarity constraint  $U(t)U(t)^\dagger = I$  with respect to  $t$  at  $t = 0$  yields

$$U\dot{U}(0)^\dagger + \dot{U}(0)U^\dagger = 0. \quad (\text{A2})$$

Letting the tangent vector be  $\eta := \dot{U}(0)$ , the above condition implies  $(\eta U^\dagger)^\dagger = -(\eta U^\dagger)$ . Hence, the matrix  $\Omega := \eta U^\dagger$  is skew-Hermitian. Consequently, the tangent space at  $U$  is defined as

$$T_U = \{\Omega U : \Omega^\dagger = -\Omega\} = \mathfrak{u}(N)U. \quad (\text{A3})$$

Here,  $\mathfrak{u}(N)$  denotes the Lie algebra of the unitary group, consisting of all  $N \times N$  skew-Hermitian matrices and closed under the Lie bracket  $[X, Y] = XY - YX$ . In particular, at the identity  $I \in U(N)$ , we have  $T_I = \mathfrak{u}(N)$ . Since  $\dim \mathfrak{u}(N) = N^2$ , the manifold  $U(N)$  has dimension  $N^2$ . Note that the tangent spaces of the unitary group differ only through right multiplication by  $U$ .

#### 2. Riemannian gradient

Consider a function  $f : U(N) \subseteq \mathbb{C}^{N \times N} \rightarrow \mathbb{R}$ . The Euclidean gradient  $\nabla f(U)$  gives the direction of steepest ascent in the ambient space  $\mathbb{C}^{N \times N}$ , but it generally does

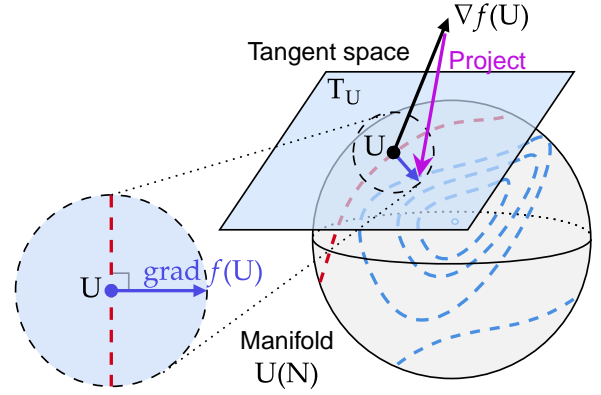


**Figure 5:** Riemannian gradient on the manifold.

Viewing  $U(N)$  as a sphere for illustration, the

Riemannian gradient  $\text{grad } f(U)$  is the orthogonal projection of the Euclidean gradient  $\nabla f(U)$  onto the tangent space at  $U$ . It is perpendicular to the contour and points in the direction of the fastest increase of  $f$ .

not lie in the tangent space  $T_U$  and thus is not a feasible direction on the manifold. The standard approach is to orthogonally project the Euclidean gradient onto  $T_U$  (see [23, Proposition 3.61]); the resulting tangent vector is called the *Riemannian gradient*,  $\text{grad } f(U) \in T_U$ . Geometrically, the Riemannian gradient is perpendicular to the contour line of  $f$  passing through  $U$  (see Fig. 5).

Here, we equip all tangent spaces  $T_U$  with the Frobenius inner product  $\langle A, B \rangle = \text{Tr}(A^\dagger B)$ , which is the metric inherited from the ambient space  $\mathbb{C}^{N \times N}$ . The normal space at  $U \in U(N)$  is defined as the orthogonal complement of the tangent space:

$$N_U := \{Z \in \mathbb{C}^{N \times N} : \langle Z, X \rangle = 0, \forall X \in T_U\}. \quad (\text{A4})$$

Algebraically, this space can be characterized as

$$N_U = \{MU : M^\dagger = M\} = \mathcal{H}(N)U, \quad (\text{A5})$$

where  $\mathcal{H}(N)$  is the space of  $N \times N$  Hermitian matrices.

Using the orthogonal decomposition  $\mathbb{C}^{N \times N} = T_U \oplus N_U$ , any  $Z \in \mathbb{C}^{N \times N}$  can be written as  $Z = (\Omega + M)U$ , where  $\Omega^\dagger = -\Omega$  and  $M^\dagger = M$ . Multiplying by  $U^\dagger$  on the right gives  $ZU^\dagger = \Omega + M$ . Taking the skew-Hermitian part yields  $\Omega = \text{Skew}(ZU^\dagger)$  with  $\text{Skew}(A) := \frac{1}{2}(A - A^\dagger)$ . Hence, the orthogonal projection of  $Z$  onto  $T_U$  is

$$\mathcal{P}_U(Z) := \text{Skew}(ZU^\dagger)U. \quad (\text{A6})$$

The Riemannian gradient is then  $\text{grad } f(U) = \mathcal{P}_U(\nabla f(U))$ .

For the cost function  $f(U) = \text{Tr}(HU\psi_0U^\dagger)$ , the Euclidean gradient is  $\nabla f(U) = 2HU\psi_0$ . In general, if  $A$  and  $B$  are (skew-)Hermitian, then  $\text{Skew}(2AB) = [A, B]$ . Applying this identity with  $A := H$  and  $B := U\psi_0U^\dagger$ , and using Eq. (A6), we obtain

$$\text{grad } f(U) = \text{Skew}(2HU\psi_0U^\dagger)U = [H, U\psi_0U^\dagger]U, \quad (\text{A7})$$

We denote the left skew-Hermitian factor by  $\widetilde{\text{grad}}f(U) := [H, U\psi_0U^\dagger] \in \mathfrak{u}(N)$ .

### 3. Retractions

Standard additive updates  $U + t\eta$  leave the unitary manifold  $U(N)$ , as they violate the unitarity constraint. To map such updates back onto  $U(N)$  while preserving the search direction, one introduces a geometric mapping called a *retraction* [21, 38], which is a central tool in the modern manifold optimization framework.

Define  $TU(N) := \{(U, \eta) : U \in U(N), \eta \in T_U\}$ . A retraction on  $U(N)$  is a smooth mapping

$$R : TU(N) \rightarrow U(N), \quad (U, \eta) \mapsto R_U(\eta), \quad (\text{A8})$$

such that for any  $U \in U(N)$  and  $\eta \in T_U$ , the induced curve  $t \mapsto \gamma(t) := R_U(t\eta)$  satisfies

$$\gamma(0) = U \text{ and } \dot{\gamma}(0) = \eta. \quad (\text{A9})$$

For the unitary manifold  $U(N)$ , several retractions are available. Given  $U \in U(N)$  and a tangent vector  $\eta = \tilde{\eta}U \in T_U$  with  $\tilde{\eta} \in \mathfrak{u}(N)$ , common retractions include:

1. Riemannian exponential map [24]:

$$R_U^{\text{exp}}(\eta) = \exp(\tilde{\eta})U, \quad (\text{A10})$$

which generates the exact geodesic curves on  $U(N)$ .

2. (First-order) Trotter retraction [31, 43, 53]:

$$R_U^{\text{trt}}(\eta) = \left( \prod_{j=1}^{N^2} \exp(i\omega^j P^j) \right) U, \quad (\text{A11})$$

where  $\tilde{\eta} \in \mathfrak{u}(N)$  is expanded in the  $\log_2(N)$ -qubit Pauli basis  $\{P^j\}_{j=1}^{N^2}$  as  $\tilde{\eta} = i \sum_j \omega^j P^j$  for  $\omega^j \in \mathbb{R}$ .

3. Cayley transform retraction [54]:

$$R_U^{\text{cay}}(\eta) = \left( I - \frac{1}{2}\tilde{\eta} \right)^{-1} \left( I + \frac{1}{2}\tilde{\eta} \right) U. \quad (\text{A12})$$

4. QR decomposition retraction [21]:

$$R_U^{\text{qr}}(\eta) = \text{qf}(U + \eta), \quad (\text{A13})$$

where  $\text{qf}(A)$  denotes the orthogonal  $Q$ -factor in the QR decomposition of  $A$ .

5. Polar decomposition retraction [21]:

$$R_U^{\text{polar}}(\eta) = (U + \eta)(I + \eta^\dagger \eta)^{-1/2}, \quad (\text{A14})$$

where  $(I + \eta^\dagger \eta)^{-1/2}$  is the inverse of the unique positive definite Hermitian square root of  $I + \eta^\dagger \eta$ .

The effectiveness of these retractions strongly depends on the computational paradigm. The Riemannian exponential map and the Trotter retraction correspond to physical Hamiltonian evolution, making them naturally suited for implementation on quantum hardware; however, their reliance on matrix exponentials renders them computationally inefficient on classical computers. Conversely, the Cayley, QR, and polar retractions rely on matrix inversions and factorizations. While implementing these nonlinear operations on quantum circuits incurs additional overhead, they are highly optimized within numerical linear algebra, making them the preferred choice in classical computing environments.

### 4. Riemannian Hessian

Unlike the usual setting, where the Hessian is represented by a symmetric matrix of second-order partial derivatives, the Riemannian Hessian at  $U$ , denoted by  $\text{Hess}f(U)$ , is a self-adjoint linear operator on  $T_U$ . It describes the covariant derivative of the Riemannian gradient field along a tangent direction, thereby naturally incorporating both the second-order variation of the objective function and the curvature of the manifold.

For the objective  $f(U) = \text{Tr}(HU\psi_0U^\dagger)$ , evaluating the Riemannian Hessian along a tangent direction  $\Omega U \in T_U$  yields the explicit formula (see Lemma 2):

$$\text{Hess}f(U)[\Omega U] = \frac{1}{2} \left( [H, [\Omega, \psi]] + [[H, \Omega], \psi] \right) U, \quad (\text{A15})$$

where  $\psi := U\psi_0U^\dagger$  is the density operator of the current quantum state. This linear operator can be equivalently represented by its action directly on  $\mathfrak{u}(N)$ :

$$\widetilde{\text{Hess}}f(U)[\Omega] = \frac{1}{2} \left( [H, [\Omega, \psi]] + [[H, \Omega], \psi] \right). \quad (\text{A16})$$

A derivation of this Hessian expression can be found in [31, Proposition 1]. To verify the correctness of Eq. (A16), we will apply the second-order Taylor expansion on  $U(N)$ . For  $\eta = \Omega U \in T_U$ , using the Riemannian exponential retraction  $R_U(\eta) = e^{\Omega}U$  in Eq. (A10), we obtain

$$\begin{aligned} & f(R_U(t\eta)) \\ &= f(U) + t \langle \widetilde{\text{grad}}f(U), \eta \rangle + \frac{t^2}{2} \langle \text{Hess}f(U)[\eta], \eta \rangle + \mathcal{O}(t^3), \\ &= f(U) + t \langle \widetilde{\text{grad}}f(U), \Omega \rangle + \frac{t^2}{2} \langle \widetilde{\text{Hess}}f(U)[\Omega], \Omega \rangle + \mathcal{O}(t^3). \end{aligned} \quad (\text{A17})$$

The updated unitary matrix is defined by  $U(t) := R_U(t\eta) = e^{t\Omega}U$ . The corresponding perturbed quantum state, represented by the density operator, is given by

$$\psi(t) = U(t)\psi_0U(t)^\dagger = (e^{t\Omega}U)\psi_0(e^{t\Omega}U)^\dagger \quad (\text{A18})$$

$$= e^{t\Omega}(U\psi_0U^\dagger)e^{-t\Omega} = e^{t\Omega}\psi_0e^{-t\Omega}. \quad (\text{A19})$$

Expanding this state to the second order in  $t$  yields

$$\begin{aligned}\psi(t) &= \left(I + t\Omega + \frac{t^2}{2}\Omega^2\right) \psi \left(I - t\Omega + \frac{t^2}{2}\Omega^2\right) + \mathcal{O}(t^3) \\ &= \psi + t[\Omega, \psi] + \frac{t^2}{2}[\Omega, [\Omega, \psi]] + \mathcal{O}(t^3).\end{aligned}\quad (\text{A20})$$

Substituting  $R_U(t\eta)$  into the cost function gives

$$\begin{aligned}f(R_U(t\eta)) &= f(U(t)) = \text{Tr}(H\psi(t)) \\ &= \text{Tr}(H\psi) + t\text{Tr}(H[\Omega, \psi]) + \frac{t^2}{2}\text{Tr}(H[\Omega, [\Omega, \psi]]) + \mathcal{O}(t^3).\end{aligned}\quad (\text{A21})$$

$$\quad (\text{A22})$$

Note that the zeroth-order term  $f(U) = \text{Tr}(H\psi)$ . Thus, the remaining task is to verify that the first- and second-order coefficients in Eq. (A17) and Eq. (A22) coincide.

For the first-order coefficient in Eq. (A17), since  $\widetilde{\text{grad}}f(U) = [H, \psi]$ , we have

$$\langle \widetilde{\text{grad}}f(U), \Omega \rangle = -\text{Tr}([H, \psi]\Omega) = \text{Tr}(H[\Omega, \psi]), \quad (\text{A23})$$

where the last equality follows from the identity

$$\text{Tr}([A, B]C) = \text{Tr}(A[B, C]) \quad (\text{A24})$$

for arbitrary  $A, B, C$ . Therefore, this coefficient coincides with that in Eq. (A22).

For the second-order coefficient in Eq. (A17), we have

$$\langle \widetilde{\text{Hess}}f(U)[\Omega], \Omega \rangle = -\text{Tr}(\widetilde{\text{Hess}}f(U)[\Omega]\Omega) \quad (\text{A25})$$

$$= -\frac{1}{2}\text{Tr}\left(\underbrace{[H, [\Omega, \psi]]\Omega}_{a:=} + \underbrace{[[H, \Omega], \psi]\Omega}_{b:=}\right). \quad (\text{A26})$$

Using Eq. (A24), the traces of  $a, b$  can be evaluated as

$$\begin{aligned}\text{Tr}([H, [\Omega, \psi]]\Omega) &= \text{Tr}(H[[\Omega, \psi], \Omega]) = -\text{Tr}(H[\Omega, [\Omega, \psi]]), \\ \text{Tr}([[H, \Omega], \psi]\Omega) &= \text{Tr}([H, \Omega][\psi, \Omega]) = -\text{Tr}(H[\Omega, [\Omega, \psi]]).\end{aligned}$$

Substituting these expressions into Eq. (A26) yields

$$\langle \widetilde{\text{Hess}}f(U)[\Omega], \Omega \rangle = \text{Tr}(H[\Omega, [\Omega, \psi]]), \quad (\text{A27})$$

which matches the second-order Taylor coefficient in Eq. (A22), thereby verifying the Riemannian Hessian formula of Eq. (A16).

In general manifold optimization, computing a Newton step necessitates the computationally expensive inversion of this Hessian operator. However, as demonstrated in Theorem 3, when the Hamiltonian is a projector ( $H = H^2$ ), the Riemannian gradient strictly emerges as an exact eigenvector of this Hessian operator.

## Appendix B: Proofs

*Proof of Theorem 3.* Substituting  $g = [H, \psi]$  into the definition of  $L$  yields

$$L(g) = \frac{1}{2}([H, [g, \psi]] + [[H, g], \psi]). \quad (\text{B1})$$

By Jacobi identity  $[A, [B, C]] = [[A, B], C] + [B, [A, C]]$ , applied with  $A = H, B = g$ , and  $C = \psi$ , we obtain

$$[H, [g, \psi]] = [[H, g], \psi] + [g, g] = [[H, g], \psi]. \quad (\text{B2})$$

Therefore,  $L(g) = [[H, g], \psi]$ . Next, since  $H^2 = H$ , we compute

$$[H, g] = [H, [H, \psi]] = [H, H\psi - \psi H] \quad (\text{B3})$$

$$= H\psi - 2H\psi H + \psi H. \quad (\text{B4})$$

Hence,  $[[H, g], \psi] = [H\psi - 2H\psi H + \psi H, \psi]$ . Using  $\psi^2 = \psi$  and  $\psi H\psi = q\psi$ , we evaluate the three terms separately:

$$[H\psi, \psi] = H\psi - q\psi, \quad [\psi H, \psi] = q\psi - \psi H, \quad (\text{B5})$$

$$[H\psi H, \psi] = qH\psi - q\psi H. \quad (\text{B6})$$

Combining these identities yields

$$[[H, g], \psi] = (H\psi - q\psi) - 2(qH\psi - q\psi H) + (q\psi - \psi H) \quad (\text{B7})$$

$$= (1 - 2q)(H\psi - \psi H) = (1 - 2q)g. \quad (\text{B8})$$

Thus,  $L(g) = (1 - 2q)g$ . This completes the proof.  $\square$

- 
- [1] M. Grassl, B. Langenberg, M. Roetteler, and R. Steinwandt, Applying Grover's algorithm to AES: quantum resource estimates, in *Post-Quantum Cryptography, Lecture Notes in Computer Science*, Vol. 9606 (Springer, 2016) pp. 29–43.
- [2] D. J. Bernstein, Post-quantum cryptography, in *Encyclopedia of Cryptography, Security and Privacy* (Springer, 2025) pp. 1846–1847.
- [3] C. Durr and P. Hoyer, A quantum algorithm for finding the minimum, arXiv preprint quant-ph/9607014 10.48550/arXiv.quant-ph/9607014 (1996).
- [4] A. Gilliam, S. Woerner, and C. Gocciulea, Grover adap-

tive search for constrained polynomial binary optimization, *Quantum* **5**, 428 (2021).

- [5] D. Dong, C. Chen, H. Li, and T.-J. Tarn, Quantum reinforcement learning, *IEEE Transactions on Systems, Man, and Cybernetics, Part B (Cybernetics)* **38**, 1207 (2008).
- [6] Y. Du, M.-H. Hsieh, T. Liu, and D. Tao, A Grover-search based quantum learning scheme for classification, *New Journal of Physics* **23**, 023020 (2021).
- [7] C. H. Bennett, E. Bernstein, G. Brassard, and U. Vazirani, Strengths and weaknesses of quantum computing, *SIAM Journal on Computing* **26**, 1510 (1997).
- [8] D. E. Knuth, *The Art of Computer Programming, Vol-*

- ume 3: *Sorting and Searching*, 2nd ed., Vol. 3 (Addison-Wesley, Reading, Massachusetts, 1998).
- [9] C. D. Manning, P. Raghavan, and H. Schütze, *Introduction to Information Retrieval* (Cambridge University Press, 2008).
- [10] L. K. Grover, A fast quantum mechanical algorithm for database search, in *Proceedings of the twenty-eighth annual ACM symposium on Theory of computing* (1996) pp. 212–219.
- [11] M. A. Nielsen and I. L. Chuang, *Quantum Computation and Quantum Information* (Cambridge University Press, 2010).
- [12] C. Zalka, Grover’s quantum searching algorithm is optimal, *Physical Review A* **60**, 2746 (1999).
- [13] R. Beals, H. Buhrman, R. Cleve, M. Mosca, and R. De Wolf, Quantum lower bounds by polynomials, *Journal of the ACM (JACM)* **48**, 778 (2001).
- [14] G. Brassard, P. Hoyer, M. Mosca, and A. Tapp, Quantum amplitude amplification and estimation, arXiv preprint quant-ph/0005055 10.48550/arXiv.quant-ph/0005055 (2000).
- [15] Y. Suzuki, S. Uno, R. Raymond, T. Tanaka, T. Onodera, and N. Yamamoto, Amplitude estimation without phase estimation, *Quantum Information Processing* **19**, 75 (2020).
- [16] A. Gilyén, Y. Su, G. H. Low, and N. Wiebe, Quantum singular value transformation and beyond: exponential improvements for quantum matrix arithmetics, in *Proceedings of the 51st Annual ACM SIGACT Symposium on Theory of Computing* (2019) pp. 193–204.
- [17] J. M. Martyn, Z. M. Rossi, A. K. Tan, and I. L. Chuang, Grand unification of quantum algorithms, *PRX Quantum* **2**, 040203 (2021).
- [18] A. Miyake and M. Watati, Geometric strategy for the optimal quantum search, *Physical Review A* **64**, 042317 (2001).
- [19] C. Cafaro and S. Mancini, On Grover’s search algorithm from a quantum information geometry viewpoint, *Physica A: Statistical Mechanics and its Applications* **391**, 1610 (2012).
- [20] Y. Suzuki, M. Gluza, J. Son, B. H. Tiang, N. H. Ng, and Z. Holmes, Grover’s algorithm is an approximation of imaginary-time evolution, arXiv preprint 10.48550/arXiv.2507.15065 (2025), arXiv:2507.15065.
- [21] P.-A. Absil, R. Mahony, and R. Sepulchre, *Optimization Algorithms on Matrix Manifolds* (Princeton University Press, 2008).
- [22] J. Hu, X. Liu, Z.-W. Wen, and Y.-X. Yuan, A brief introduction to manifold optimization, *Journal of the Operations Research Society of China* **8**, 199 (2020).
- [23] N. Boumal, *An Introduction to Optimization on Smooth Manifolds* (Cambridge University Press, 2023).
- [24] B. C. Hall, *Lie Groups, Lie Algebras, and Representations: An Elementary Introduction*, 2nd ed., Graduate Texts in Mathematics, Vol. 222 (Springer International Publishing Switzerland, 2015) pp. XIII + 449.
- [25] M.-C. Hsu, E.-J. Kuo, W.-H. Yu, J.-F. Cai, and M.-H. Hsieh, Quantum state tomography via nonconvex Riemannian gradient descent, *Physical Review Letters* **132**, 240804 (2024).
- [26] Z.-T. Li, X.-L. He, C.-C. Zheng, Y.-Q. Dong, T. Luan, X.-T. Yu, and Z.-C. Zhang, Quantum comb tomography via learning isometries on Stiefel manifold, *Physical Review Letters* **134**, 010803 (2025).
- [27] R. Wiersema and N. Killoran, Optimizing quantum circuits with Riemannian gradient flow, *Physical Review A* **107**, 062421 (2023).
- [28] A. B. Magann, S. E. Economou, and C. Arenz, Randomized adaptive quantum state preparation, *Physical Review Research* **5**, 033227 (2023).
- [29] E. Malveti, C. Arenz, G. Dirr, and T. Schulte-Herbrüggen, Randomized gradient descents on Riemannian manifolds: Almost sure convergence to global minima in and beyond quantum optimization, arXiv preprint arXiv:2405.12039 10.48550/arXiv.2405.12039 (2024).
- [30] M. Pervez, A. Haqq, N. A. McMahon, and C. Arenz, Riemannian gradient descent-based quantum algorithms for ground state preparation with guarantees, arXiv preprint arXiv:2512.13401 10.48550/arXiv.2512.13401 (2025).
- [31] Z. Lai, H. Nie, J. Wu, and D. An, Quantum circuit design from a retraction-based Riemannian optimization framework, arXiv preprint arXiv:2602.20605 10.48550/arXiv.2602.20605 (2026).
- [32] A. Kotil, R. Banerjee, Q. Huang, and C. B. Mendl, Riemannian quantum circuit optimization for Hamiltonian simulation, *Journal of Physics A: Mathematical and Theoretical* **57**, 135303 (2024).
- [33] I. N. M. Le, S. Sun, and C. B. Mendl, Riemannian quantum circuit optimization based on matrix product operators, *Quantum* **9**, 1833 (2025).
- [34] I. Luchnikov, A. Ryzhov, S. Filippov, and H. Ouerdane, QGOpt: Riemannian optimization for quantum technologies, *SciPost Physics* **10**, 079 (2021).
- [35] I. A. Luchnikov, M. E. Krechetov, and S. N. Filippov, Riemannian geometry and automatic differentiation for optimization problems of quantum physics and quantum technologies, *New Journal of Physics* **23**, 073006 (2021).
- [36] Y. Yao, F. Miatto, and N. Quesada, Riemannian optimization of photonic quantum circuits in phase and Fock space, *SciPost Physics* **17**, 082 (2024).
- [37] Z. Lai, D. An, J. Hu, and Z. Wen, A Grover-compatible manifold optimization algorithm for quantum search, arXiv preprint arXiv:2512.08432 10.48550/arXiv.2512.08432 (2025).
- [38] R. L. Adler, J.-P. Dedieu, J. Y. Margulies, M. Martens, and M. Shub, Newton’s method on Riemannian manifolds and a geometric model for the human spine, *IMA Journal of Numerical Analysis* **22**, 359 (2002).
- [39] P. Kaye, R. Laflamme, and M. Mosca, *An Introduction to Quantum Computing* (Oxford University Press., 2006).
- [40] G. Brassard, Searching a quantum phone book, *Science* **275**, 627 (1997).
- [41] L. K. Grover, Fixed-point quantum search, *Physical Review Letters* **95**, 150501 (2005).
- [42] T. J. Yoder, G. H. Low, and I. L. Chuang, Fixed-point quantum search with an optimal number of queries, *Physical Review Letters* **113**, 210501 (2014).
- [43] H. F. Trotter, On the product of semi-groups of operators, *Proceedings of the American Mathematical Society* **10**, 545 (1959).
- [44] J. E. Dennis Jr and R. B. Schnabel, *Numerical Methods for Unconstrained Optimization and Nonlinear Equations* (SIAM, 1996).
- [45] C. T. Kelley, *Solving Nonlinear Equations with Newton’s method* (SIAM, 2003).
- [46] J. Nocedal and S. J. Wright, *Numerical Optimization* (Springer, 2006).
- [47] O. P. Ferreira and R. C. Silva, Local convergence of New-

- ton's method under a majorant condition in Riemannian manifolds, *IMA Journal of Numerical Analysis* **32**, 1696 (2012).
- [48] A. Peruzzo, J. McClean, P. Shadbolt, M.-H. Yung, X.-Q. Zhou, P. J. Love, A. Aspuru-Guzik, and J. L. O'Brien, A variational eigenvalue solver on a photonic quantum processor, *Nature Communications* **5**, 4213 (2014).
- [49] A. Kandala, A. Mezzacapo, K. Temme, M. Takita, M. Brink, J. M. Chow, and J. M. Gambetta, Hardware-efficient variational quantum eigensolver for small molecules and quantum magnets, *Nature* **549**, 242 (2017).
- [50] W. Huang, K. A. Gallivan, and P.-A. Absil, A Broyden class of quasi-Newton methods for Riemannian optimization, *SIAM Journal on Optimization* **25**, 1660 (2015).
- [51] W. Huang, P.-A. Absil, and K. A. Gallivan, A Riemannian BFGS method without differentiated retraction for nonconvex optimization problems, *SIAM Journal on Optimization* **28**, 470 (2018).
- [52] Z. Lai, GroverNewton public codes, <https://github.com/GALVINLAI/GroverNewton> (2026), accessed: 2026-3-20.
- [53] S. Lloyd, Universal quantum simulators, *Science* **273**, 1073 (1996).
- [54] Z. Wen and W. Yin, A feasible method for optimization with orthogonality constraints, *Mathematical Programming* **142**, 397 (2013).